Bond Activation in Iron(II) and Nickel(II) Complexes of Polypodal Phosphanes

Simon-Andreas Gentschow[a], Stephan W. Kohl[a], Walter Bauer[b], Frank W. Heinemann[c], Dennis Wiedemann[a], and Andreas Grohmann[a]

[a] Technische Universität Berlin, Institut für Chemie, Straße des 17. Juni 135, 10623 Berlin, Germany
[b] Universität Erlangen-Nürnberg, Department Chemie und Pharmazie, Organische Chemie, Henkestraße 42, 91054 Erlangen, Germany
[c] Universität Erlangen-Nürnberg, Department Chemie und Pharmazie, Anorganische Chemie, Egerlandstraße 1, 91058 Erlangen, Germany

Reprint requests to Prof. Dr. A. Grohmann. E-mail: andreas.grohmann@chem.tu-berlin.de

*Dedicated to Professor Rolf W. Saalfrank on the occasion of his 70th birthday*

A pyridine-derived tetraphosphane ligand (donor set: NP$_4$) has been found to undergo remarkably specific C–P bond cleavage reactions, thereby producing a ligand with an NP$_3$ donor set. The reaction may be reversed under suitable conditions, with regeneration of the original NP$_4$ ligand. In order to investigate the mechanism of this reaction, the NP$_3$ donor ligand C$_5$H$_3$N[CMe(CH$_2$PMe$_2$)$_2$][CMe$_2$(CH$_2$PMe$_2$)] (**11**) was prepared, and its iron(II) complex **4** generated from Fe(BF$_4$)$_2 \cdot$ 6 H$_2$O, with methyl diethylphosphinite (**7**) as an additional monodentate ligand. Ligand **11** has, in addition to the NP$_3$ donor set, one methyl group in close contact with the iron center, reminiscent of an agostic M$\cdots$H–C interaction. Depending on the stoichiometric amount of iron(II) salt, a side product **15** is formed, which has a diethylphosphane ligand instead of the phosphinite **7** coordinated to iron(II). While attempts to deprotonate the metal-coordinated methyl group in **4** were unsuccessful, the reaction was shown to occur in an alternative complex (**18**), which is similar to **4** but has a trimethylphosphane ligand instead of the phosphinite **7**. The reaction of complex **15** with CO gave two different products, which were both characterized by single-crystal X-ray diffraction. One (**19**) is the dicarbonyl iron(II) complex of the triphosphane ligand **11**, the other (**3**) is the carbonyl iron(II) complex of the tetraphosphane C$_5$H$_3$N[CMe(CH$_2$PMe$_2$)$_2$]$_2$ (**1**). This suggests an *inter*molecular mechanism for the C–P bond formation in question.

Key words: Bond Activation, N/P Ligands, Polypodal Ligands, Agostic Interaction, Iron, Nickel

Introduction

Homogeneous catalysts are often transition metal complexes with tertiary phosphane ligands (*e. g.*, Wilkinson's catalyst [1]). A known decomposition reaction in such complexes is intramolecular C–H bond activation, the best known example being orthometalation of a phenyl ring in *aryl*phosphane ligands [2]. The reaction proceeds by insertion of the metal into a C–H bond of the ligand, and usually deactivates the catalyst. A less frequently observed type of side reaction is metal insertion into a C–P bond of the ligand, sometimes initiated by the solvent, which acts as a nucleophile [3]. We recently described what appears to be the first solvent-induced C–P bond cleavage in an *alkyl*phosphane ligand [4, 5]. As outlined in Scheme 1, complex formation between

Fe(BF$_4$)$_2 \cdot$ 6 H$_2$O and the pyridine-derived tetrapodal tetraphosphane **1** in methanol proceeds with solvent-induced cleavage of one C–PMe$_2$ bond. Depending on the reaction temperature, two different products are observed: treatment of **1** with a stoichiometric amount of the iron(II) salt in methanol at room temperature leads to complex **2b**, which has a methyl group in agostic interaction with the iron center, while the analogous procedure at −50 °C forms complex **2a**, which contains a carbanionic methylene group. In both cases, a monodentate phosphinite ligand Me$_2$P(OMe), formed from the cleaved PMe$_2$ group and methanol, completes the coordination octahedron. While treatment of **2b** with CO does not lead to any well-defined products, compound **2a**, under analogous conditions, reacts unexpectedly with reversion of the previous P–C bond cleavage. This restores the original pentadentate
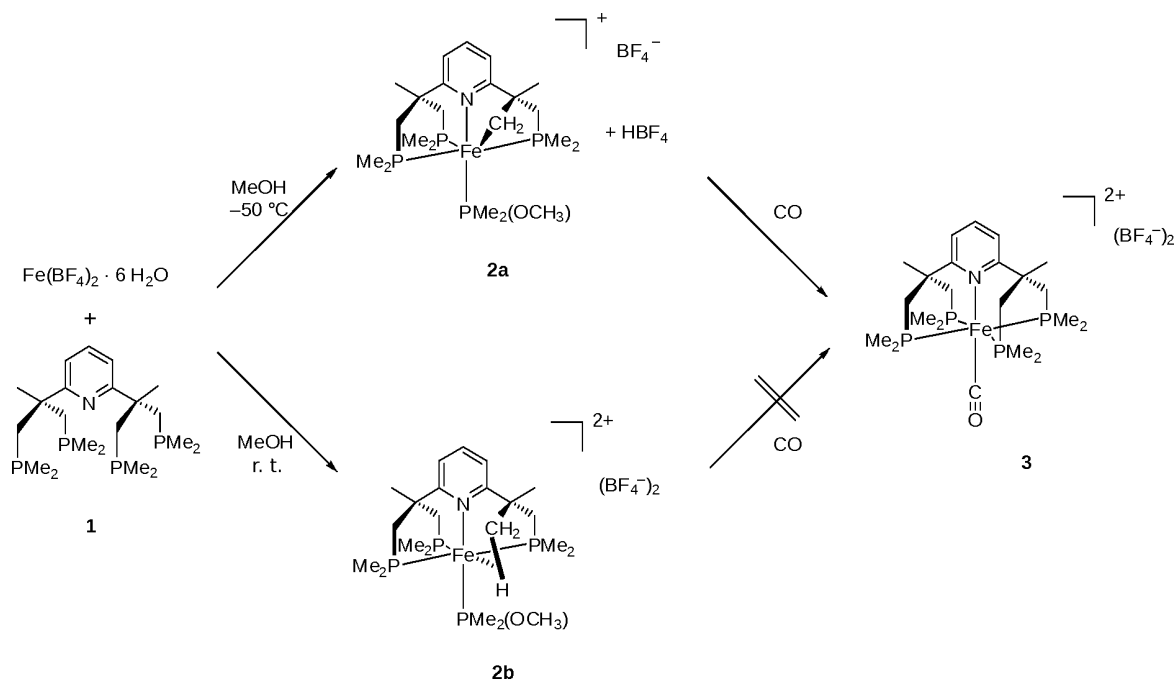
Scheme 1. P–C bond breaking and remaking reactions involving the pyridine-derived tetraphosphane ligand **1**.
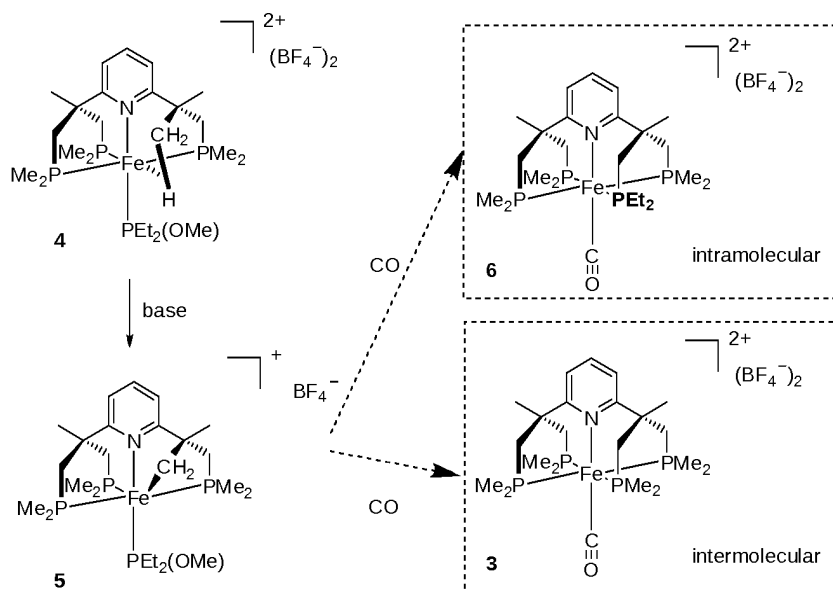
Scheme 2. Most likely products (boxes) of the reaction of **5** with CO, depending on whether the reaction follows an *intra-* or *inter*molecular pathway.

NP$_4$ ligand, giving complex **3**. In terms of mechanism, the process may be *intra*molecular (and thereby entail breaking a P–O bond in the phosphinite ligand which is expected to be strong) or *inter*molecular (requiring transfer of a PMe$_2$ unit from a sacrificial second molecule of the starting complex).

In order to elucidate the mechanism of this reaction, we attempted to synthesize a "carbanionic" complex similar to **2a**, differing only in the phosphinite ligand. Instead of methyl di*methyl*phosphinite, we aimed to introduce a methyl di*ethyl*phosphinite ligand (complex **4** in Scheme 2). If a tetrapodal pen-

tadentate phosphane ligand was to be produced from this complex upon reaction with CO, in the same way as shown in Scheme 1, we reasoned that for an *intra*molecular process, the new NP_4 ligand would contain a di*ethyl*phosphanyl group in the place of one of the di*methyl*phosphanyl groups in **1** (complex **6** in Scheme 2) whereas, if complex **3** was detected, the reaction would undoubtedly follow an *inter*molecular pathway.

As complex **5** is not accessible along the route that produces complex **2a**, we chose to prepare the permethylated triphosphane ligand $C_5H_3N[CMe(CH_2PMe_2)_2][CMe_2(CH_2PMe_2)]$ (**11**), hoping to obtain **4** from its complexation reaction with iron(II) tetrafluoroborate hexahydrate in the presence of 1 eq. methyl diethylphosphinite (**7**). Deprotonation of **4** was then expected to provide access to the carbanionic ligand complex **5**.

Results and Discussion

The required P ligands were synthesized in a first step. Methyl diethylphosphinite (**7**) was prepared in good yield (88 %) from the reaction of equimolar amounts of chlorodiethylphosphane, triethylamine and methanol in pentane (Scheme 3).

The preparation of **11** followed the synthetic route shown in Scheme 4. Unlike the route to tetraphosphane **1** [4, 6, 7], the synthesis of triphosphane **11** starts from 2-ethyl-6-isopropyl-pyridine (which we prepared as described by Wakatsuki and Yamazaki [8]). Hydroxymethylation of the reactive α-carbon atoms with aqueous formaldehyde
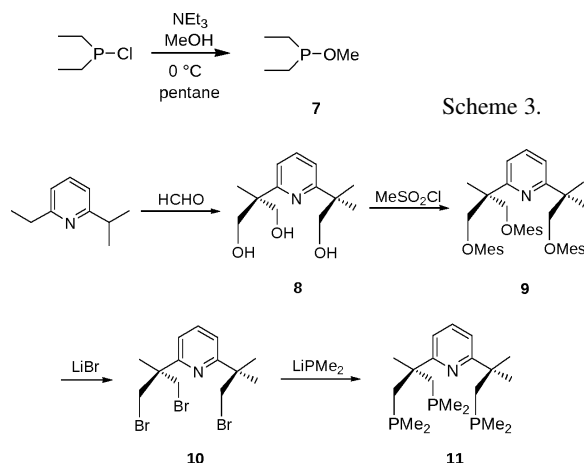
Scheme 3.

Scheme 4. Synthesis of the triphosphane **11** (stereochemical representation arbitrary).
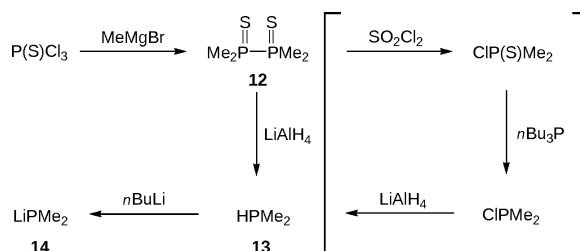
Scheme 5. Previous [9] (including compounds in brackets) and modified synthetic route to LiPMe$_2$ (**14**).

in an autoclave at 140 °C yielded the trialcohol $C_5H_3N[CMe(CH_2OH)_2][CMe_2(CH_2OH)]$ (**8**) as a colorless solid. The three pyridine protons show as an ABC system in the ^{1}H-NMR spectrum of **8** [δ = 7.66 ppm (t, ^3J(H,H) = 7.9 Hz, 1 H, py-H^3), 7.20 ppm (d, ^3J(H,H) = 8.0 Hz, 1 H, py-H^2), 7.17 ppm (d, ^3J(H,H) = 8.0 Hz, 1 H, py-H^4)]. The hydroxyl groups give rise to a broad signal at 4.14 ppm.

Whereas the preparation of **1** involves clean tosylation of the corresponding tetraalcohol, tosylation of the trialcohol does not proceed cleanly. Attempted reactions of **8** using the combinations TsCl/NaOH/THF/H_2O, TsCl/KOH/THF and TsCl/NEt$_3$/dichloromethane gave only about 12 % of the desired product, plus several types of unwanted chlorides. We therefore prepared the trimesylate $C_5H_3N[CMe(CH_2OMes)_2][CMe_2(CH_2OMes)]$ (**9**) by reaction of **8** with methanesulfonyl chloride and triethylamine in dichloromethane (yield: 93 %). **9** was then treated with lithium bromide at 70 °C in DMSO to give the tribromide $C_5H_3N[CMe(CH_2Br)_2]$-$[CMe_2(CH_2Br)]$ (**10**). In the last step, **10** was subsequently reacted with lithium dimethylphosphide in diethyl ether at −78 °C, producing **11**. The ^{31}P{^{1}H}-NMR spectrum of the product shows two singlets with a ratio of 2 : 1 at −62.06 and −61.84 ppm for the non-equivalent P atoms of the dimethylphosphanyl groups. In the ^{1}H-NMR spectrum, there again is an ABC spin system (t, d, d), due to the three pyridine protons, and the non-equivalent *ortho*-carbon atoms of the pyridine ring give rise to two signals (167.5 ppm, 165.8 ppm) in the ^{13}C{^{1}H}-NMR spectrum.

The established route to lithium dimethylphosphide (**14**) [9, 10] starts from thiophosphoryl chloride and goes through five reaction steps ending in the conversion of dimethylphosphane with *n*-butyllithium [11] (Scheme 5). We were able to introduce a shortcut into the reaction sequence by converting tetramethyldiphosphane disulfide (**12**)
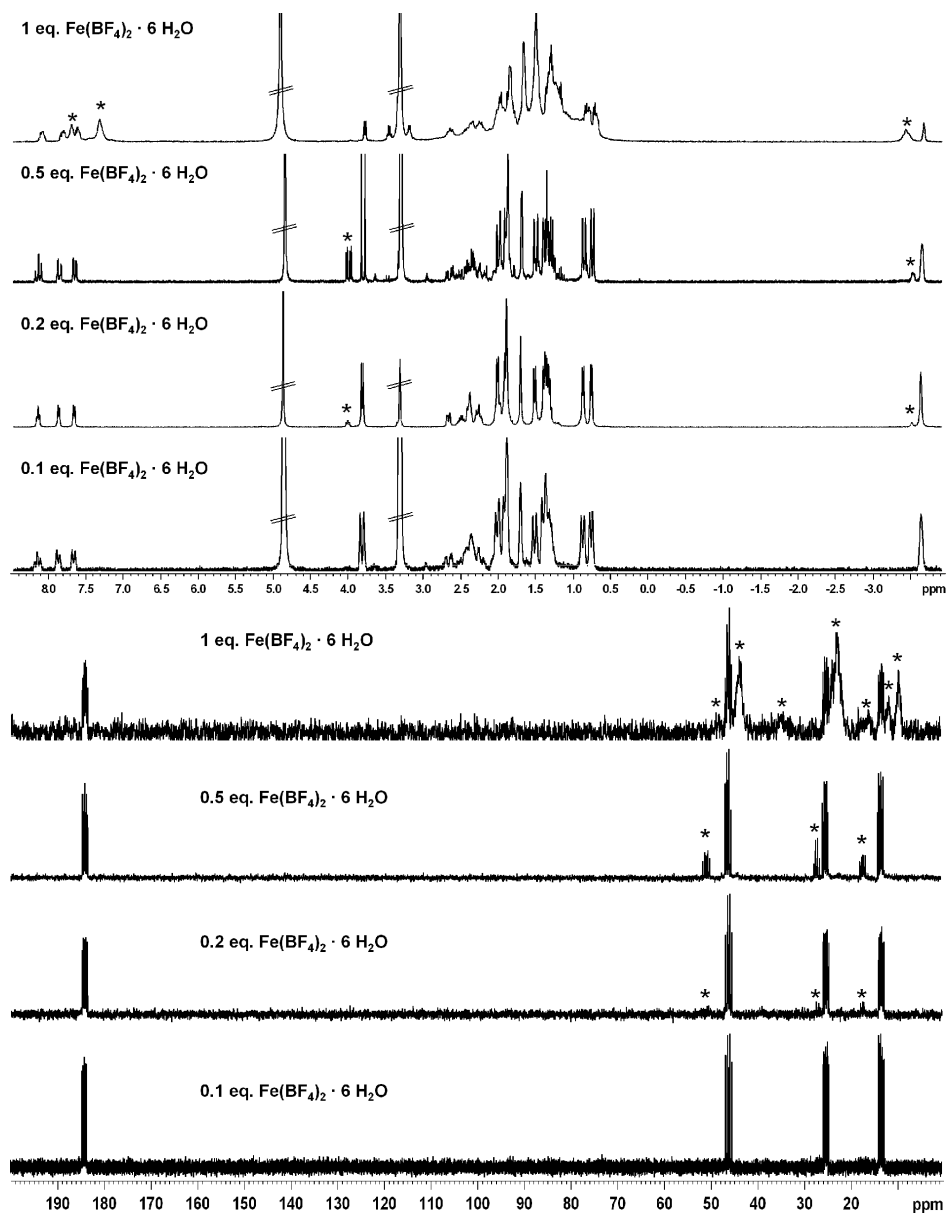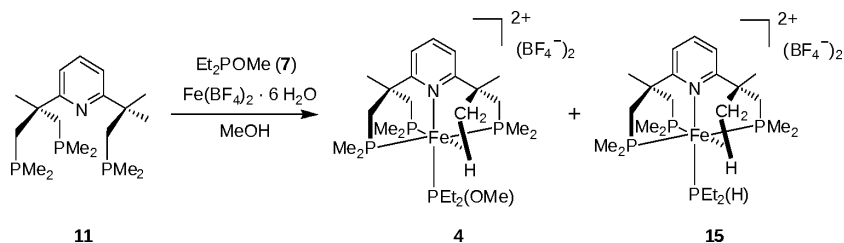
Fig. 1. Increase of side products in the complexation reaction producing **4** as a function of the amount of iron(II) salt employed (^{1}H-, ^{31}P-NMR spectra; signals due to side products marked with asterisks).
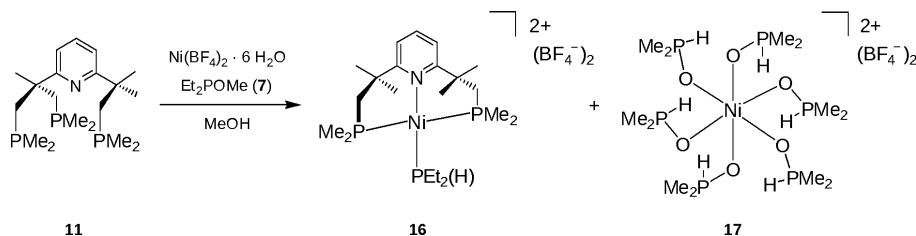
directly into two equivalents of dimethylphosphane (**13**) [12, 13], thereby avoiding the preparation of chlorodimethylphosphane sulfide and chlorodimethylphosphane, and at the same time increasing the yield of **13** from 37 % to 83 % (based on tetramethyldiphosphane disulfide; see Scheme 5).

The subsequent complexation reaction of the triphosphane **11** with $Fe(BF_4)_2 \cdot 6\,H_2O$ in the presence of 1 eq. **7** produced complex **4**. To our surprise, however, the selectivity of the reaction depends strongly on the amount of iron(II) salt employed. The ^{1}H- and ^{31}P-NMR traces summarized in Fig. 1 clearly demonstrate the correlation between the stoichiometry (amount of $Fe(BF_4)_2 \cdot 6\,H_2O$ used) and the formation of pure product **4**: only the desired complex **4** is formed when the ratio of **11** : **7** : iron(II) salt is 1 : 1 : 0.1. Most significantly, there is a prominent and slightly broadened signal at high field (−3.7 ppm) in the ^{1}H-NMR spectrum, which is characteristic of the methyl group in close contact with the metal center. The broadening

Et$_2$POMe (7)
Fe(BF$_4$)$_2$ · 6 H$_2$O
MeOH

11   4   15   Scheme 6.

Ni(BF$_4$)$_2$ · 6 H$_2$O
Et$_2$POMe (7)
MeOH

11   16   17

Scheme 7. P–C bond breaking involving the triphosphane ligand **11** at nickel(II).

is presumably due to rotation of the methyl group, which is relatively slow on the NMR time scale. A doublet assignable to the phosphinite ligand is located at 3.82 ppm. The three protons on the pyridine ring show up as an ABC spin system (triplet, doublet, doublet) between *ca.* 7.6 and 8.2 ppm, as is characteristic for this asymmetrical molecule. The region between *ca.* 0.7 and 3.0 ppm shows the partially overlapping signals due to the six PMe$_2$ groups, two methyl groups and the three methylene groups. In the ^{31}P-NMR spectrum, there is a total of four signals. The signal at about 184 ppm is characteristic of the coordinated phosphinite, and the other three signals, between *ca.* 10 and 50 ppm, are due to the coordinated triphosphane.

The more the amount of iron(II) salt used in the reaction is increased, the more we observe the formation of an unexpected side product, with diagnostic signals both in the ^{1}H- and ^{31}P-NMR spectra (Fig. 1; signals labeled with an asterisk). This product is expected to be very similar to the desired product **4**, because it apparently also contains a methyl group in the vicinity of the metal center (a second signal of growing intensity appears in the ^{1}H-NMR spectrum at high field), and it apparently also contains the ligand **11** (there is a second set of three signals in the ^{31}P-NMR spectrum between 10 to 50 ppm, whose intensity increases as the proportion of iron salt is increased in the reaction). Finally, the reaction of *equimolar* amounts of **11**, **7** and iron salt seems to give more than one side product, and both the ^{1}H-NMR and the ^{31}P-NMR spectra show broadened signals.

Isothermal diffusion of diethyl ether into a solution of the product mixture obtained from the reac-

tion with 0.5 equivalents of iron salt in methanol gave dark-purple crystals of this side product (complex **15** in Scheme 6). While the crystals were of insufficient quality for a full structure determination, the obtained data allowed unambiguous clarification of the connectivity in the complex. As deduced from the NMR spectroscopic data, it contains the triphosphane ligand **11**, with one methyl group in contact with the metal. Unlike complex **4**, however, the monodentate P ligand at the sixth coordination site is diethylphosphane instead of methyl diethylphosphinite.

Apparently, when the amount of iron(II) salt is increased, the reaction proceeds, at least in part, with reduction of the phosphinite to a phosphane. Interestingly, this reduction is not confined to iron(II) as the central metal, as a control experiment showed it to occur also when reacting the triphosphane **11** with phosphinite **7** and *nickel*(II) tetrafluoroborate hexahydrate in methanol (Scheme 7). Isothermal diffusion of diethyl ether into a solution of the crude reaction product in DMSO gave orange single crystals. Preliminary X-ray data established the connectivity and allowed identification of the product **16** and, separately, **17**. Two details about this reaction merit particular mention.

Firstly, the reaction converts methyl diethylphosphinite to diethylphosphane, which is coordinated to nickel(II). We are at this stage unable to offer an explanation as to how this reduction proceeds. Similar reactions in the literature use metal hydrides [14] or Birch conditions (Li solvated in NH$_3$) [15]. It could be speculated that in our case insertion of the metal center into a C–H bond of the phosphane lig-
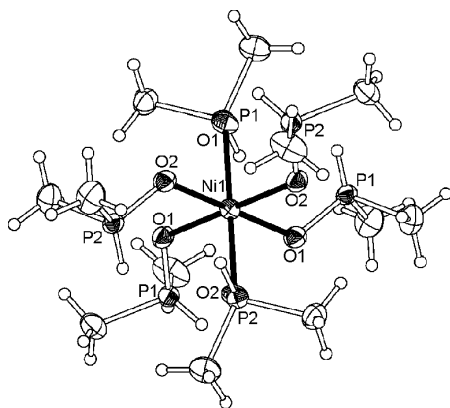
Fig. 2. Molecular structure of the dicationic nickel(II) complex in **17** in the crystal (only heteroatoms labeled for clarity).

Table 1. Bond lengths (Å) and angles (deg) in the nickel(II) dication of **17** (standard deviations in parentheses).

Ni1–O1	2.044(4)
Ni1–O2	2.066(3)
O1–Ni1–O1	91.0(2), 91.0(2), 91.0(2)
O1–Ni1–O2	86.5(2), 90.5(2), 177.1(2)
O2–Ni1–O2	92.1(2), 92.1(2), 92.1(2)

11   **18**
Scheme 8.

and could produce a metal hydride, which could then transfer H^- to the phosphorus atom, to yield diethylphosphane. This process would, however, require oxidative addition at nickel(II), which appears unlikely, as the hydride ligand is not expected to tolerate high nickel oxidation states. Secondly, the conversion entails another C–P bond breaking event, as **16** is a square-planar nickel(II) complex in which the newly formed NP$_2$ ligand $C_5H_3N[CMe_2(CH_2PMe_2)]_2$ ("py(PMe$_2$)$_2$") occupies three coordination sites, and newly formed diethylphosphane the fourth. This activation is most probably initiated by solvate water of the nickel(II) precursor. In a parallel experiment in methanol, isothermal diffusion of diethyl ether into a solution of the crude reaction product gave green-yellow single crystals. The X-ray structure analysis has revealed a nickel(II) complex of octahedral symmetry (**17**), whose structure is shown in Fig. 2. Apparently, water (or hydroxide) cleaves a PMe$_2$ group to produce dimethylphosphinous acid, Me$_2$P(OH), six equivalents of which coordinate, in the form of the more stable dimethylphosphane oxide tautomer, to a nickel(II) center. All phosphorus-bonded H atoms were located as electron density residuals in difference Fourier maps at meaningful distances and angles relative to their respective P carrier atoms.

Table 1 gives a selection of bond lengths and angles. The crystal system is trigonal (space group *P*31*c*, *Z* = 2). All Ni–O distances are in the expected range, with values between 2.04 and 2.07 Å [16]. The coordination geometry at nickel(II) is quite regular.
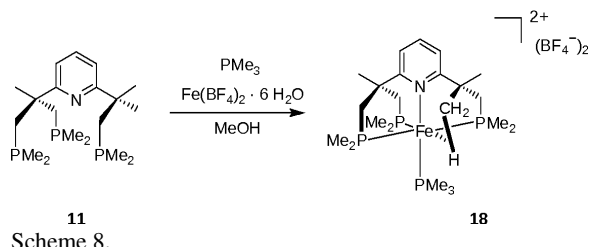
Despite varied efforts, deprotonation of complex **4** to give complex **5** could not be achieved, owing to lability of the phosphinite ligand towards bases, as monitored by NMR spectroscopy: the addition of base causes the signals assigned to the phosphinite group to disappear almost instantaneously, and the reaction leads to undefined products. We therefore decided to synthesize a complex similar to **4** but with a monodentate phosphane ligand which we expected to be inert towards base. We sought to determine whether such a complex, with a methyl group in close (agostic) interaction with the metal atom, could be deprotonated at all. The reaction of equimolar amounts of triphosphane ligand **11**, iron(II) salt and trimethylphosphane as co-ligand in methanol gave pure complex **18** in 86 % yield (Scheme 8).

Its ^{1}H-NMR spectrum (Fig. 3) resembles the spectrum of **4**. The pyridine protons give rise to an ABC system (triplet, doublet, doublet) between *ca.* 7.6 and 8.2 ppm (see enlargement at left). The signal of the agostic methyl group is located at −3.48 ppm. The enlargement at right shows six doublets for the three inequivalent PMe$_2$ groups (each having a pair of diastereotopic Me groups), the doublet for the PMe$_3$ group and the proton signals for the methyl and methylene groups. The integrated intensities of all signals are as expected.

The ^{31}P-NMR spectrum (Fig. 4) shows four signals. The signal at *ca.* 15 ppm belongs to the coordinated PMe$_3$ ligand, and the other three signals belong to the three PMe$_2$ groups of the triphosphane ligand. For a more precise interpretation of the signals we simulated the experimental spectrum. As shown in Fig. 4, agreement is excellent.
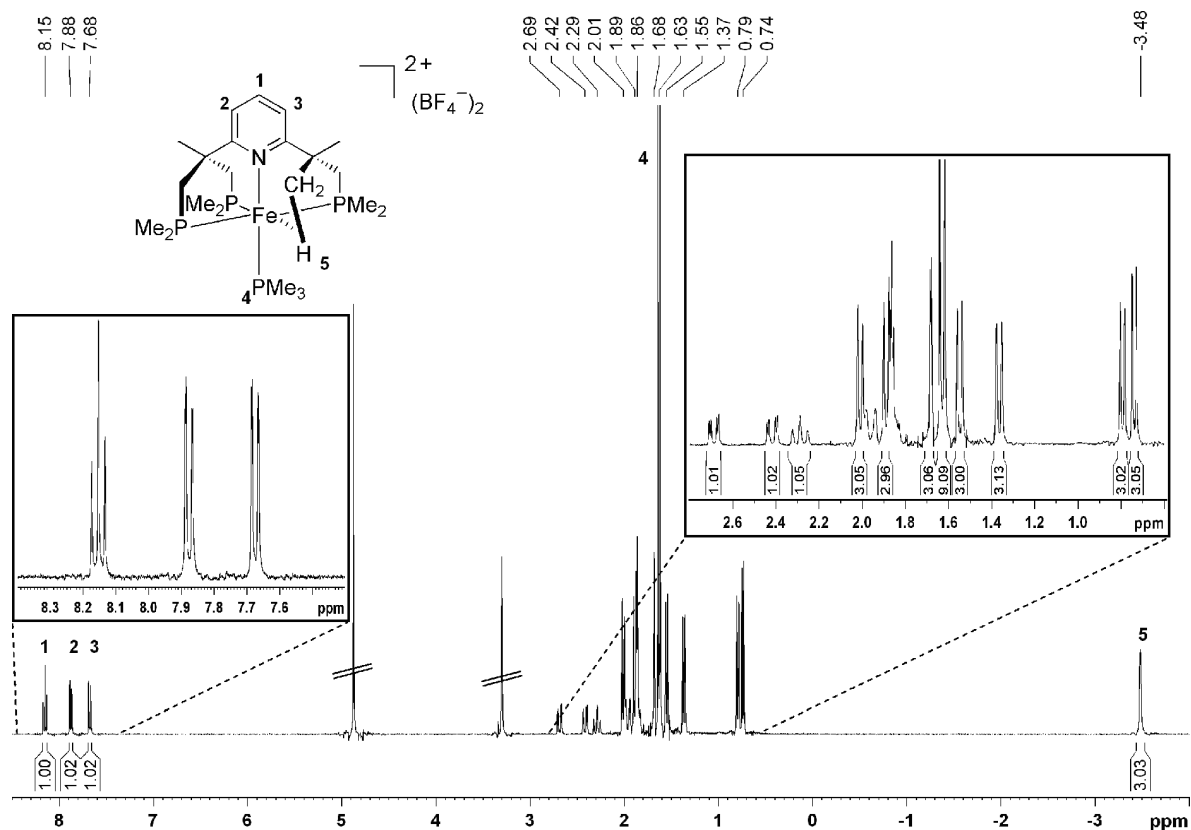
Fig. 3. ^{1}H-NMR spectrum ([D$_4$]methanol]) of complex **18**.

Table 2. Coupling constants (in Hz) in the ^{31}P-NMR spectrum of **18**.

	Chemical shifts (ppm)	P2	P3	P4	P1
P2	45.98 (a)	–	–	–	–
P3	23.40 (b)	−58.22 (ab)	–	–	–
P4	15.07 (c)	−69.82 (ac)	+39.33 (bc)	–	–
P1	14.34 (d)	−65.17 (ad)	−78.55 (bd)	+37.29 (cd)	–

The extracted coupling constants (in Hz) with their relative signs are listed in Table 2. The true signs are unknown.

The trimethylphosphane ligand does confer sufficient stability on complex **18** with respect to the reaction with base, and ^{1}H-NMR data indicate the deprotonation of the methyl group to proceed as desired: The signal of the agostic methyl group can be made disappear almost completely, while two new doublets appear at 0.20 and 0.54 ppm, characteristic of the complex in which a carbanionic methylene group is coordinated directly to the iron(II) center [4]. The ^{31}P-NMR spectrum also shows the signals expected for the de-

sired product. However, all attempts at its purification failed, and complex **18** was thus unavailable for the intended mechanistic study.

As an alternative, we reacted complex **15** with excess CO, reasoning that reduction of CO (to give formaldehyde) could transform, by dehydrogenation, complex **15** into a more reactive species. The reaction, which was performed in EtOH in an autoclave at 65 °C over 4 h with a CO pressure of 10 bar, produced a yellow solid. Isothermal diffusion of diethyl ether into a solution of the solid in acetonitrile and methanol gave two kinds of single crystals (orange-yellow and yellow), which were suitable for analysis by single-crystal X-ray diffraction. The crystals represent complexes **19** and **3** (Scheme 9).

19 is the product of replacement of the agostic methyl group and of the diethylphosphane ligand by two equivalents of CO (Fig. 5). Complex **3**, which contains the original tetraphosphane ligand **1**, should only be accessible by an *inter*molecular reaction, in which the fourth PMe$_2$ group is provided by a second equiv-
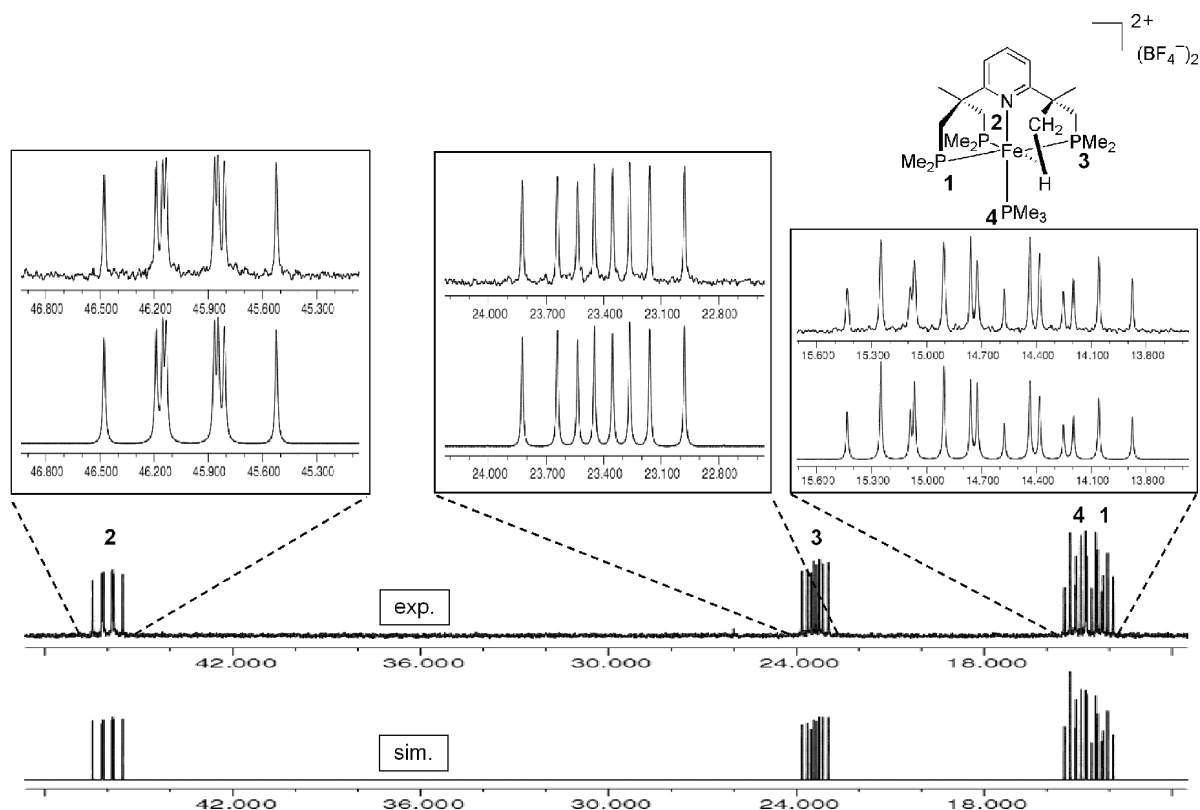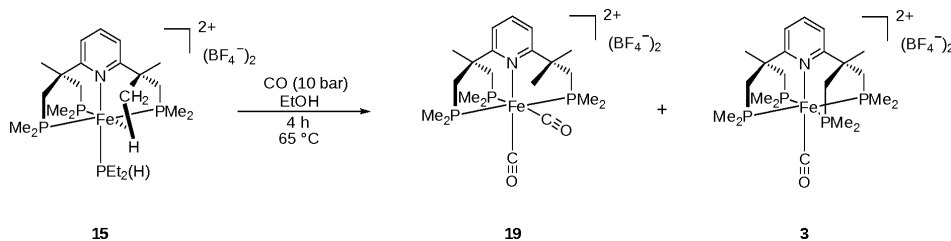
Fig. 4. Comparison of the experimental and simulated ^{31}P-NMR spectra of **18**.

Scheme 9. Two of the products of the reaction of **15** with excess CO, as ascertained by single-crystal X-ray analysis.

alent of complex. The NP$_3$P$'$ ligand that would be produced in an *intra*molecular reaction, containing one PEt$_2$ group, has not been found. Future work aims to elucidate the exact mechanism of this reaction, and will entail careful determination of yields in all cases.

Table 3 lists selected bond lengths and angles in **19**. The coordination geometry at iron(II) is distorted octahedral. One of the two carbonyl ligands is *trans* to the nitrogen atom of the pyridine ring, and the other is *trans* to P2, thereby giving a *cis*-dicarbonyliron moiety. Due to phosphorus being a better donor than nitrogen, the bond Fe1–C21 is longer than the bond Fe1–C20. The two arrangements N1–Fe–C20–O1 (N1–Fe–C20

176.44(16)°, Fe1–C20–O1 178.5(4)°) and P2–Fe1–C21–O2 (P2–Fe1–C21 173.53(13)°, Fe1–C21–O2 178.6(4)°) are essentially linear. The iron-phosphorus and iron-nitrogen distances in this dicarbonyl complex are generally longer than in other complexes of ligand **11**, as formed by C–P bond cleavage [4, 5].

The crystal structure of complex **3** is equivalent to that of the monocarbonyl complex obtained by the reaction of **2a** with CO, published in 2006 [4]. The coordination geometry at iron(II) is a severely distorted octahedron, as expressed by the values of the nitrogen-iron-phosphorus angles, which alternate between 80° and 100°. The pyridine-iron-carbonyl fragment (N1–

Table 3. Bond lengths (Å) and angles (deg) in the dication of **19** · 0.5 MeCN (standard deviations in parentheses).

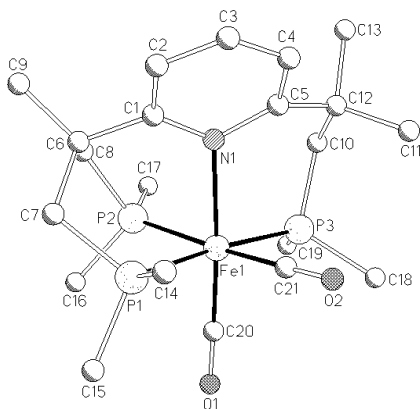| Fe1–N1	2.166(3)	Fe1–P1	2.300(2)
Fe1–P2	2.267(2)	Fe1–P3	2.255(2)
Fe1–C20	1.752(4)	Fe1–C21	1.812(4)
N1–Fe1–C20	176.4(2)	N1–Fe1–C21	88.5(2)
Fe1–C20–O1	178.5(4)	Fe1–C21–O2	178.6(4)
P1–Fe1–P3	173.29(4)	P2–Fe1–C20	90.6(2)
P2–Fe1–C21	173.5(2)		

Fig. 5. Molecular structure of the dication in **19** · 0.5 MeCN in the crystal.

Fe1–C22 177.55(8)°, Fe1–C22–O1 177.5(2)°) in this monocarbonyl complex is again linear. The Fe–P and the Fe–N distances are in good agreement with other iron(II) complexes of **1** [5].

Conclusion

The mechanism underlying the formation of the tetraphosphane ligand **1** in the reaction of **2a** with CO remains elusive, owing to the lability of complex **5** towards base. The deprotonation of a methyl group forced into close proximity to the metal is possible, however, as shown for complex **18**, gives a product with a direct Fe–C bond. The synthesis of the phosphinite complex **4** is accompanied by reduction of the phosphinite ligand to a phosphane ligand. This side reaction becomes more prominent as the amount of iron(II) salt is increased. Its product is complex **15**, which has a diethylphosphane ligand coordinated to iron(II), in addition to the triphosphane **11**. The reaction of complex **15** with CO gave the dicarbonyl iron(II) complex **19** and the monocarbonyl complex **3** as well-defined products. The formation of the latter suggests an *inter*molecular reaction mechanism for the generation of the tetraphosphane ligand.

Experimental Section

Materials and instrumentation

Unless noted otherwise, all reactions were carried out at r. t. in dried solvents under dry dinitrogen using standard Schlenk techniques. $Fe(BF_4)_2 \cdot 6\,H_2O$ and $Ni(BF_4)_2 \cdot 6\,H_2O$ were purchased from Aldrich and used without further purification. Carbon monoxide (99.997 %) was purchased from Air Liquide.

IR spectra of solids were measured as KBr disks and assigned on the basis of literature data [17]. Spectroscopic data were obtained with the following instruments: IR spectroscopy: Nicolet Magna System 750; mass spectrometry: Varian 311 A and Spektrospin CMS FT-ICR; NMR spectroscopy: Bruker ARX 200 and Bruker ARX 400. Signs of coupling constants in the ^{1}H, ^{13}C and ^{31}P spectra were not determined. The superscripts for NMR assignments follow the numbering scheme adopted for the X-ray crystal structure of **19** · 0.5 MeCN. Elemental analyses were carried out with a Thermo Finnigan, Flash EA, 1112 Series analyzer.

[Fe(**1**)CO](BF₄)₂ (**3**)

A suspension of **15** (125 mg, 0.181 mmol) in ethanol (8 mL) was reacted during 4 h with CO (10 bar) in an autoclave at 65 °C. The color of the solid changed from purple to yellow. The autoclave was allowed to cool to room temperature, opened, and the suspension transferred into an empty flask. The ethanol was then removed by syringe. The remaining yellow powder was washed with diethyl ether (2×3 mL) and dried *in vacuo*. Isothermal diffusion of diethyl ether into a solution of the material in methanol gave a small crop of single crystals of **3**.

[Fe(**11**)(CH₃)(Et₂POMe)](BF₄)₂ (**4**)

A solution of $Fe(BF_4)_2 \cdot 6\,H_2O$ (36 mg, 0.106 mmol) in methanol (3 mL) was added dropwise to a solution of **11** (394 mg, 1.06 mmol) and **7** (0.191 mL, 1.06 mmol, 10 eq.) in methanol (4 mL), giving a purple solution. The mixture was stirred for 30 min, then diethyl ether (10 mL) was added, and a purple powder precipitated. The powder was filtered off and washed with methanol (3×1 mL). It was dried *in vacuo* yielding purple microcrystals (35 mg, 0.05 mmol, 46 %). – ^{1}H NMR (200 MHz, [D₄]methanol, r. t.): δ = 8.18 (t, ^3J(H,H) = 8.0 Hz, 1 H, py-H^3), 7.90 (d, ^3J(H,H) = 8.6 Hz, 1 H, py-H^2), 7.68 (d, ^3J(H,H) = 8.0 Hz, 1 H, py-H^4), 3.82 (m, 3 H, POCH_3), 2.68, 2.34 (m/m, 2 H, C$H_2{}^7$), 2.61, 2.24 (m/m, 2 H, C$H_2{}^8$), 2.48, 2.18 (m/m, 2 H, C$H_2{}^{10}$), 2.46 – 2.13 (br, 4 H, 2× PCH_2), 1.99 (m, 3 H, PC$H_3{}^{16}$), 1.88 (m, 3 H, PC$H_3{}^{17}$), 1.86 (s, 3 H, C$H_3{}^9$), 1.68 (s, 3 H, C$H_3{}^{11}$), 1.48 (m, 3 H, PC$H_3{}^{18}$), 1.37 (m, 3 H, PC$H_3{}^{19}$), 1.29 (t, ^2J(H,H) = 5.5 Hz, 6 H, 2× PCH₂CH_3), 0.84 (m, 3 H, PC$H_3{}^{14}$), 0.73 (m, 3 H, PC$H_3{}^{15}$), −3.71 (s, 3 H, C$H_3{}^{13}$) ppm. –

$^{31}P\{^1H\}$ NMR (161.97 MHz, [D$_4$]methanol, r. t.): δ = 184.69 (m, PEt_2OMe), 46.37 (m, P^2), 25.59 (m, P^3), 13.59 (m, P^1) ppm. – ^{13}C NMR (100.64 MHz, [D$_4$]methanol, r. t.): δ = 170.64 (s, py-C^5), 169.13 (s, py-C^1), 142.74 (s, py-C^3), 124.41 (s, py-C^4), 123.96 (s, py-C^2), 55.99 (m, POCH$_3$), 44.91 (s, CCH$_3{}^6$), 44.52 (s, CCH$_3{}^{12}$), 43.46 (m, CH$_2{}^{10}$), 38.49 (m, CH$_2{}^7$), 35.76 (m, CH$_2{}^8$), 32.28 (m, PCH$_2$), 31.45 (m, PCH$_2$), 28.32 (m, CH$_3{}^9$), 27.26 (m, CH$_3{}^{11}$), 25.36 (m, CH$_3{}^{13}$), 23.27 (m, PCH$_3{}^{18}$), 18.40 (m, PCH$_3{}^{19}$), 16.57 (m, PCH$_3{}^{14}$), 16.29 (m, PCH$_3{}^{15}$), 15.03 (m, PCH$_3{}^{16}$), 14.75 (m, PCH$_3{}^{17}$), 9.02 (m, PCH$_2$CH$_3$) ppm. – IR (KBr): $\tilde{\nu}$ = 2974s, 2931s, 1575s, 1464s, 1309s, 1057vs (BF$_4{}^-$), 1030s, 939s, 913s, 762s cm^{-1}. – C$_{24}$H$_{49}$B$_2$F$_8$FeNOP$_4$ (721.00): calcd. C 39.98, H 6.85, N 1.94; found C 40.18, H 6.46, N 2.04.

Methyl diethylphosphinite (7)

A solution of chlorodiethylphosphane (2.00 g, 0.016 mol) in pentane (15 mL) was added to a solution of triethylamine (2.32 mL, 0.016 mol) and methanol (0.66 mL, 0.016 mol) in pentane (10 mL) over 45 min at 0 °C. The resulting triethyl-ammonium chloride was filtered off, and the solvent was removed from the filtrate by distillation. The crude product can be purified by distillation (b. p.: 124 – 126 °C, 1013 mbar). The product is a colorless liquid (1.66 g, 88 %). – ^{1}H NMR (200 MHz, [D$_1$]chloroform, r. t.): δ = 3.45 (d, ^3J(P,H) = 14.7 Hz, 3 H, OCH$_3$), 1.50 (m, 4 H, CH$_2$), 1.03 (m, 6 H, CH$_3$) ppm. – ^{31}P NMR (161.97 MHz, [D$_1$]chloroform, r. t.): δ = 140.88 (s, PMe$_2$) ppm.

C$_5$H$_3$N[CMe(CH$_2$OH)$_2$][CMe$_2$(CH$_2$OH)] (8)

An autoclave (volume: 2.1 L) was charged with 2-ethyl-6-isopropyl pyridine (50 g, 0.33 mol) and aqueous formalde-hyde solution (37 %, stabilized with 10 % methanol, 250 mL, 3.30 mol), and the mixture heated to 140 °C for 48 h. The mixture was allowed to cool to r. t., the autoclave opened, and water removed from the reaction mixture under reduced pressure at 60 °C. Excess formaldehyde was removed by dry-ing the yellow syrupy liquid for 24 h at 100 °C *in vacuo*. The residue was taken up in chloroform (250 mL) and extracted with water (30 × 70 mL). The combined water extracts were brought to dryness under reduced pressure, and the residue dried for another 48 h at 95 °C *in vacuo*. After trituration with diethyl ether (200 mL), the product was obtained as a colorless powder, which was filtered off and dried *in vacuo* (27.7 g, 35 %). – ^{1}H NMR (400 MHz, [D$_1$]chloroform, r. t.): δ = 7.66 (t, ^3J(H,H) = 7.9 Hz, 1 H, H^3), 7.20 (d, ^3J(H,H) = 8.0 Hz, 1 H, H^2), 7.17 (d, ^3J(H,H) = 8.0 Hz, 1 H, H^4), 4.14 (br, 3 H, OH), 3.92 – 3.75 (dd, AB, ^2J(H,H) = 11.2 Hz, 4 H, $H^{7,8}$), 3.66 (s, 2 H, H^{10}), 1.29 (s, 6 H, $H^{11,13}$), 1.17 (s, 3 H, H^9) ppm. – ^{13}C NMR (100.64 MHz, [D$_1$]chloroform, r. t.): δ = 165.23 (s, 1 C, C^1), 163.27 (s, 1 C, C^5), 137.56 (s, 1 C, C^3), 118.95 (s, 1 C, C^2), 118.66 (s, 1 C, C^4), 71.83 (s, 1 C,

C^{10}), 69.38 (s, 2 C, $C^{7,8}$), 45.97 (s, 1 C, C^6), 42.01 (s, 1 C, C^{12}), 24.95 (s, 2 C, $C^{11,13}$), 19.89 (s, 1 C, C^9) ppm. – IR (KBr): $\tilde{\nu}$ = 3299vs (OH), 2961vs, 2873vs, 1577vs, 1461vs, 1042vs, 1027vs, 756s cm^{-1}. – EI-MS (70 eV): *m/z* (%) = 239 (100) [M]$^+$. – C$_{13}$H$_{21}$NO$_3$ (239.31): calcd. C 65.25, H 8.84, N 5.75; found C 64.97, H 8.80, N 5.67.

C$_5$H$_3$N[CMe(CH$_2$OMes)$_2$][CMe$_2$(CH$_2$OMes)] (9)

A solution of methanesulfonyl chloride (12.8 mL, 0.166 mol) in dichloromethane (50 mL) was added drop-wise to a solution of **8** (11.0 g, 0.046 mol) and triethylamine (29.2 mL, 0.207 mol) in dichloromethane (200 mL) at −2 °C. The mixture was allowed to warm to r. t. and stirred for 1 h. After washing with HCl (1 N, 50 mL), water (50 mL), sat-urated aqueous Na$_2$CO$_3$ (50 mL), brine (50 mL), and again water (50 mL), the dichloromethane phase was separated and dried over Na$_2$SO$_4$. The solvent was removed under reduced pressure, and the residue dried *in vacuo* to give a light-yellow oil (20.3 g, 93 %). – ^{1}H NMR (200 MHz, [D$_1$]chloroform, r. t.): δ = 7.70 (t, ^3J(H,H) = 8.0 Hz, 1 H, H^3), 7.27 (d, ^3J(H,H) = 7.9 Hz, 1 H, H^2), 7.21 (d, ^3J(H,H) = 7.9 Hz, 1 H, H^4), 4.63 – 4.52 (dd, AB, ^2J(H,H) = 8.8 Hz, 4 H, $H^{7,8}$), 4.47 (s, 2 H, H^{10}), 2.96 (s, 6 H, SO$_2$-CH_3), 2.86 (s, 3 H, SO$_2$-CH_3), 1.50 (s, 3 H, H^9), 1.41 (s, 6 H, $H^{11,13}$) ppm. – ^{13}C NMR (50.32 MHz, [D$_1$]chloroform, r. t.): δ = 163.36 (s, 1 C, C^1), 158.42 (s, 1 C, C^5), 137.56 (s, 1 C, C^3), 119.13 (s, 1 C, C^2), 118.86 (s, 1 C, C^4), 77.64 (s, 1 C, C^{10}), 72.74 (s, 2 C, $C^{7,8}$), 45.14 (s, 1 C, C^6), 41.35 (s, 1 C, C^{12}), 36.84 (s, 2 C, SO$_2$CH$_3$), 36.74 (s, 1 C, SO$_2$CH$_3$), 24.57 (s, 2 C, $C^{11,13}$), 19.16 (s, 1 C, C^9) ppm. – IR (KBr): $\tilde{\nu}$ = 3029vs, 2976vs, 2941vs, 1578vs, 1352vs, 1172vs, 958vs, 528vs cm^{-1}. – EI-MS (70 eV): *m/z* (%) = 394 (100) [M–SO$_2$CH$_3$]$^+$.

C$_5$H$_3$N[CMe(CH$_2$Br)$_2$][CMe$_2$(CH$_2$Br)] (10)

Lithium bromide (5.17 g, 0.059 mol) was dried *in vacuo* at 100 °C for 3 d and was then added to a solution of **9** (6.27 g, 0.013 mol) in DMSO (150 mL) at 70 °C. The mixture was stirred for 2 d at this temperature and was then allowed to cool to r. t. Water (200 mL) was added, and the milky liquid stirred for another 30 min. After extraction with diethyl ether (7 × 70 mL) the combined organic phases were washed with water (3 × 50 mL) to remove excess DMSO. The ether phase was separated and dried over Na$_2$SO$_4$. The solvent was sub-sequently removed under reduced pressure and the remain-ing light-yellow oil dried *in vacuo*. Column chromatogra-phy (SiO$_2$, ethyl acetate/hexane 3 : 1) gave the product as a light-yellow oil (3.1 g, 56 %). – ^{1}H NMR (200 MHz, [D$_1$]chloroform, r. t.): δ = 7.66 (t, ^3J(H,H) = 7.9 Hz, 1 H, H^3), 7.23 (d, ^3J(H,H) = 7.9 Hz, 1 H, H^2), 7.18 (d, ^3J(H,H) = 7.9 Hz, 1 H, H^4), 4.00 – 3.86 (dd, AB, ^2J(H,H) = 10.0 Hz, 4 H, $H^{7,8}$), 3.80 (s, 2 H, H^{10}), 1.63 (s, 3 H, H^9), 1.49 (s, 6 H, $H^{11,13}$) ppm. – ^{13}C NMR (50.32 MHz, [D$_1$]chloroform, r. t.):

δ = 164.07 (s, 1 C, C^1), 160.04 (s, 1 C, C^5), 137.07 (s, 1 C, C^3), 118.48 (s, 1 C, C^2), 118.36 (s, 1 C, C^4), 46.01 (s, 2 C, $C^{6,12}$), 42.10 (s, 3 C, $C^{7,8,10}$), 26.63 (s, 2 C, $C^{11,13}$), 23.09 (s, 1 C, C^9) ppm. – IR (KBr): $\tilde{v}$ = 2969vs, 2870m, 1576vs, 1458vs, 1423m, 1247vs, 750s cm^{-1}. – EI-MS (70 eV): *m/z* (%) = 416 (32) [M–CH$_3$]$^+$, 414 (98) [M–CH$_3$]$^+$, 412 (100) [M–CH$_3$]$^+$, 410 (34) [M–CH$_3$]$^+$. – C$_{13}$H$_{18}$Br$_3$ (428.00): calcd. C 36.48, H 4.24, N 3.27; found C 36.53, H 4.40, N 3.31.

$C_5H_3N[CMe(CH_2PMe_2)_2][CMe_2(CH_2PMe_2)]$ (11)

A solution of **10** (4.2 g, 9.8 mmol) in diethyl ether (80 mL) was added dropwise to a suspension of **14** (3.6 g, 34.3 mmol) in diethyl ether at −78 °C over 2 h. The mixture was stirred overnight at r. t. The solvent was removed by distillation and the yellow residue treated with pentane (75 mL) and filtered. The solution was then brought to dryness, giving a colorless oil (2.35 g, 64 %). – ^{1}H NMR (200 MHz, [D$_1$]chloroform, r. t.): δ = 7.55 (t, ^3J(H,H) = 7.8 Hz, 1 H, py-H^3), 7.14 (d, ^3J(H,H) = 7.9 Hz, 1 H, py-H^2), 7.10 (d, ^3J(H,H) = 7.9 Hz, 1 H, py-H^4), 2.23 − 1.89 (ddd, AB, ^2J(H,H) = 10.7 Hz, ^2J(P,H) = 3.5 Hz, 4 H, $H^{7,8}$), 1.93 (d, ^2J(P,H) = 3.4 Hz, 2 H, H^{10}), 1.59 (s, 3 H, H^9), 1.45 (s, 6 H, $H^{11,13}$), 0.92 − 0.69 (3× d, ^2J(P,H) = 3.2 Hz, 18 H, 6× PCH_3^{14,15,16,17,18,19}) ppm. – ^{31}P NMR (80.95 MHz, [D$_1$]chloroform, r. t.): δ = −60.32 (s, 1× PMe$_2$), –60.47 (s, 2× PMe$_2$) ppm. – ^{13}C NMR (50.32 MHz, [D$_1$]chloroform, r. t.): δ = 167.47 (s, 1 C, py-C^1), 165.83 (s, 1 C, py-C^5), 136.81 (s, 1 C, py-C^3), 118.17 (s, 1 C, py-C^2), 117.48 (s, 1 C, py-C^4), 49.50 (m, 3 C, $C^{7,8,10}$), 44.73 (t, 1 C, C^6), 41.59 (d, 1 C, C^{12}), 29.63 (m, 2 C, $C^{11,13}$), 26.48 (m, 1 C, C^7), 16.18 (m, 6 C, PCH_3^{14,15,16,17,18,19}) ppm.

Tetramethyldiphosphane disulfide (12)

A solution of thiophosphorylchloride (33.5 mL, 0.33 mol) in diethyl ether (50 mL) was added dropwise to a solution of methylmagnesium bromide (1 mol, 3 eq.) in diethyl ether (500 mL) at −5 to −2 °C. The mixture was stirred overnight at room temperature, after which time a colorless solid had precipitated. The suspension was mixed with H$_2$O (100 mL) and was then added to a solution of concentrated H$_2$SO$_4$ (10 mL) in H$_2$O (400 mL). The mixture was stirred for 1 h. After filtration the colorless solid was washed with H$_2$O (3 × 25 mL) and diethyl ether (3 × 15 mL). It was then dried *in vacuo*, yielding the product as a colorless solid (20.9 g, 0.11 mol, 67 %). – ^{1}H NMR (200 MHz, [D$_8$]thf, r. t.): δ = 1.89 (dd, ^2J(P,H) = 12.2 Hz, ^3J(P,H) = 4.8 Hz, 12 H, CH_3) ppm. – ^{13}C NMR (100.64 MHz, [D$_1$]chloroform, r. t.): δ = 16.19 (dd, ^1J(C,P) = 60.6 Hz, ^2J(P,C) = 29.7 Hz, 4 C, CH_3) ppm. – ^{31}P NMR (80.95 MHz, [D$_8$]thf, r. t.): δ = 33.30 (s, 2× PMe$_2$) ppm. – IR (KBr): $\tilde{v}$ = 2968s, 2898s, 1402vs, 1283vs, 939vs, 882vs, 733vs (P=S), 568vs cm^{-1}. – EI-MS (70 eV): *m/z* (%) = 185 (100) [M–H]$^+$. – C$_4$H$_{12}$P$_2$S$_2$ (186.22): calcd. C 25.80, H 6.60; found C 25.44, H 6.53.

Dimethylphosphane (13)

Procedure A

A solution of chlorodimethylphosphane (4.87 g, 0.051 mmol) in diethyl ether (20 mL), cooled to 0 °C, was added to a suspension of LiAlH$_4$ (2.3 g, 0.061 mmol, 1.2 eq.) in diethyl ether (30 mL) at −78 °C. The mixture was stirred for 2 h and subsequently allowed to warm to r. t. Product and solvent were jointly distilled into an empty flask cooled with liquid N$_2$. Because of the very similar boiling points of the solvent and the product, the product could not be isolated, and the yield was not determined. The product was used without further characterization in following reactions which were calculated for 100 % yield.

Procedure B

A solution of LiAlH$_4$ (6.12 g, 0.161 mol, 2 eq.) in diethyl ether (50 mL) was added to a suspension of **12** (15 g, 0.08 mol) in diethyl ether (150 mL) over 30 min. The mixture was stirred overnight, with subsequent work-up as for Procedure **A**.

Lithium dimethylphosphide (14)

A solution of *n*-butyllithium (2.5 M solution in hexane, 65 mL, 0.161 mol) was added to a solution of **13** (9.99 g, 0.161 mmol) in diethyl ether (50 mL) at −78 °C during 2 h. The mixture was allowed to warm to r. t., depositing a colorless solid, and was stirred for 4 d at this temperature. The colorless solid was filtered off and washed with diethyl ether (3 × 20 mL). It was dried *in vacuo* to give a colorless powder (14.1 g, 0.134 mol, 83 %). – ^{1}H NMR (200 MHz, [D$_8$]thf, r. t.): δ = 1.27 (br, 6 H, CH_3) ppm. – ^{13}C NMR (50.32 MHz, [D$_8$]thf, r. t.): δ = 24.12 (d, ^1J(C,P) = 38.5 Hz, 2 C, CH_3) ppm. – ^{31}P NMR (80.95 MHz, [D$_8$]thf, r. t.): δ = −58.11 (s, PMe$_2$) ppm.

[Fe(11)(CH$_3$)(Et$_2$PH)](BF$_4$)$_2$ (15)

The procedure was the same as for the preparation of **4**, except that 0.5 eq. of Fe(BF$_4$)$_2$ · 6 H$_2$O was used instead of 0.1 eq. Isothermal diffusion of diethyl ether into a solution of the resulting purple powder gave dark-purple single crystals which were suitable for single-crystal diffraction analysis.

[Ni(Et$_2$PH)(py(PMe$_2$)$_2$)](BF$_4$)$_2$ (16)

A solution of Ni(BF$_4$)$_2$ · 6 H$_2$O (90 mg, 0.264 mmol) in methanol (2 mL) was added to a solution of **11** (98 mg, 0.264 mmol) and **7** (0.047 mL, 0.264 mmol) in methanol (3 mL). The mixture was stirred for 10 min, and an orange powder precipitated. The solution was transferred into another flask by syringe, and the remaining powder was washed

with methanol (2×2 mL) and dried *in vacuo* to yield an orange microcrystalline powder (**16**, 12 mg). An isothermal diffusion of diethyl ether into a solution of **16** in DMSO gave orange single crystals which could be analyzed by single-crystal diffraction.

[Ni{(O)P(H)Me₂}₆](BF₄)₂ (**17**)

A solution of Ni(BF₄)₂ · 6 H₂O (90 mg, 0.264 mmol) in methanol (2 mL) was added to a solution of **11** (98 mg, 0.264 mmol) and **7** (0.047 mL, 0.264 mmol) in methanol (3 mL). The mixture was stirred for 10 min, during which time an orange precipitate appeared. The mother liquor was transferred into another flask by syringe and was treated with diethyl ether to give a yellow powder. After removing the mother liquor by syringe, the powder was washed with diethyl ether (2×2 mL) an dried *in vacuo* to yield complex **17** as a yellow polycrystalline material. Isothermal diffusion of diethyl ether into a solution of **17** in methanol gave a small amount of green-yellow single crystals which were used in the single-crystal diffraction analysis.

[Fe(**11**)(CH₃)(PMe₃)](BF₄)₂ (**18**)

A solution of Fe(BF₄)₂ · 6 H₂O (98 mg, 0.29 mmol) in methanol (2 mL) was added dropwise to a solution of **11** (108 mg, 0.29 mmol) and trimethylphosphane (22 mg, 0.03 mL, 0.29 mmol) in methanol (4 mL). Stirring the mixture overnight produced a purple precipitate, which was filtered off, washed with methanol (3×2 mL), and dried *in vacuo*. Purple microcrystals (169 mg, 0.25 mmol, 86 %) were obtained. – ¹H NMR (400 MHz, [D₄]methanol, r. t.): $\delta =$ 8.15 (t, ^3J(H,H) = 7.8 Hz, 1 H, py-H^3), 7.88 (d, ^3J(H,H) = 8.5 Hz, 1 H, py-H^2), 7.68 (d, ^3J(H,H) = 8.1 Hz, 1 H, py-H^4), 2.69, 2.31 (m/m, 2 H, C$H_2{}^{10}$), 2.42, 1.98 (m/m, 2 H, C$H_2{}^7$), 2.27, 1.94 (m/m, 2 H, C$H_2{}^8$), 2.01 (m, 3 H, PC$H_3{}^{16}$), 1.89 (m, 3 H, PC$H_3{}^{17}$), 1.86 (s, 3 H, C$H_3{}^9$), 1.68 (s, 3 H, C$H_3{}^{11}$), 1.63 (d, ^2J(P,H) = 8.8 Hz, 9 H, 3× PCH_3), 1.55 (m, 3 H, PC$H_3{}^{18}$), 1.37 (m, 3 H, PC$H_3{}^{19}$), 0.79 (m, 3 H, PC$H_3{}^{14}$), 0.74 (m, 3 H, PC$H_3{}^{15}$), –3.48 (s, 3 H, C$H_3{}^{13}$) ppm. – ³¹P NMR (161.97 MHz, [D₄]methanol, r. t.): $\delta =$ 45.98 (m, P^2), 23.40 (m, P^3), 15.07 (m, PMe₃), 14.34 (m, P^1) ppm. – ¹³C NMR (100.64 MHz, [D₆]DMSO, r. t.): $\delta =$ 168.15 (s, py-C^5), 166.28 (s, py-C^1), 139.75 (s, py-C^3), 121.53 (s, py-C^4), 121.15 (s, py-C^2), 46.49 (m, C$H_2{}^8$), 42.18 (s, 2× CC$H_3{}^{6,12}$), 39.85 (m, C$H_2{}^7$), 30.20 (m, C$H_2{}^{10}$), 28.87 (s, C$H_3{}^9$), 27.91 (s, C$H_3{}^{13}$), 26.36 (s, C$H_3{}^{11}$), 20.85 (m, PC$H_3{}^{18}$), 19.71 (m, 3× PCH_3), 16.83 (m, PC$H_3{}^{19}$), 15.99 (m, PC$H_3{}^{14}$), 15.33 (m, PC$H_3{}^{16}$), 13.92 (m, PC$H_3{}^{15}$), 12.87 (m, PC$H_3{}^{17}$) ppm. – IR (KBr): $\tilde{v} =$ 2961s, 2920s, 1602m, 1462s, 1293s, 1055vs (BF₄⁻), 947s, 921s, 728s cm⁻¹. – C₂₂H₄₅B₂F₈FeNP₄ (676.95): calcd. C 39.03, H 6.70, N 2.07; found C 39.06, H 6.65, N 2.10.

Table 4. Selected crystallographic data for **17** and **19** · 0.5 MeCN.

	17	**19** · 0.5 MeCN
Molecular formula	C₁₂H₄₂B₂F₈-NiO₆P₆	C₂₂H₃₇.₅B₂F₈Fe-N₁.₅O₂P₃
M_r	700.61	677.41
Crystal size, mm³	$0.15 \times 0.14 \times 0.13$	$0.32 \times 0.18 \times 0.10$
Color	yellow	yellow
Crystal system	trigonal	monoclinic
Space group	$P31c$ (no. 159)	$P2_1$ (no. 4)
a, Å	11.7115(2)	9.995(2)
b, Å	11.7115(2)	17.367(2)
c, Å	12.4985(3)	17.904(2)
α, deg	90	90
β, deg	90	104.155(7)
γ, deg	120	90
V, Å	1484.61(5)	3013.4(5)
Z	2	4
D_c, g cm⁻³	1.57	1.49
μ, mm⁻¹	1.1	0.7
$F(000)$, e	724	1396
T, K	150(2)	150(2)
Absorption correction	SCALE 3 ABSPACK	SADABS
T_{min}/T_{max}	0.897 / 1.000	0.778 / 1.000
Scan	ω	φ and ω, 2.0° and 30 s per frame
2θ range, deg	7.0 – 57.5	6.6 – 54.2
Measured reflections	11098	54796
Unique reflections	2354	13199
Observed reflections[a]	2036	10447
Refined parameters	81	788
$wR2$ (all data)[b]	0.1723	0.1233
$R1$ (obs. data)[c]	0.0613	0.0499
Weighting scheme[d]	$k = 0.1322$ / $l = 0$	$k = 0.0733$ / $l = 0.5896$
Abs. struct. parameter	0.10(3)	0.17(2)
ρ_{fin} (max./min.), e Å⁻³	1.701 / −0.501	0.997 / −0.450

[a] With $F_o \geq 4\sigma(F)$; [b] $wR2 = [\Sigma w(F_o^2 - F_c^2)^2/\Sigma w(F_o^2)^2]^{1/2}$; [c] $R1 = \Sigma||F_o| - |F_c||/\Sigma|F_o|$; [d] $w = [\sigma^2(F_o^2) + (kP)^2 + lP]^{-1}$, where $P = (\text{Max}(F_o^2,0) + 2F_c^2)/3$.

[Fe(**11**)(CO)₂](BF₄)₂ (**19**)

A suspension of **15** (125 mg, 0.181 mmol) in ethanol (8 mL) was reacted with CO (10 bar) in an autoclave at 65 °C for 4 h. During this reaction the color of the solid changed from purple to yellow. The suspension was transferred into an empty flask and the ethanol removed by syringe. The remaining yellow powder was washed with diethyl ether (2×3 mL) and dried *in vacuo*. Isothermal diffusion of diethyl ether into a solution of the material in acetonitrile gave a small crop of single crystals of **19** which were used in the single-crystal structure determination.

Crystal structure determination

X-Ray diffraction intensity data were collected on a Bruker-Nonius KappaCCD diffractometer (**19** · 0.5 MeCN) and an Oxford Diffraction Xcalibur S Sapphire diffractome-

ter (**17**). The structures were solved by Direct Methods using SHELXTL NT 6.10 (**19** · 0.5 MeCN) and SHELXS-97 (**17**). All non-hydrogen atoms were refined anisotropically. In **19** · 0.5 MeCN, the asymmetric unit contains two independent molecules of the iron complex salt and one acetonitrile solvent molecule. Two of the four independent tetrafluoroborate counterions are disordered. In **17**, the four tetrafluoroborate counterions per unit cell occupy special positions and are highly disordered. They have consequently been treated as a diffuse contribution to the overall scattering without specific atom positions by SQUEEZE/PLATON [18]. Selected crystallographic data for **17** and **19** · 0.5 MeCN are given in Table 4.

CCDC 763852 (**17**) and CCDC 763853 (**19** · 0.5 MeCN) contain the supplementary crystallographic data for this paper. This data can be obtained free of charge from the Cambridge Crystallographic Data Center *via* www.ccdc.cam. ac.uk/data_request/cif.

[1] J. F. Young, J. A. Osborne, F. A. Jardine, G. Wilkinson *Chem. Commun.* **1965**, 131 – 132.

[2] A. D. Ryabov *Chem. Rev.* **1990**, *90*, 403 – 424.

[3] A. Caballero, F. A. Jalon, B. R. Manzano, G. Espino, M. Perez-Manrique, A. Mucientes, F. J. Poblete, M. Maestro *Organometallics* **2004**, *23*, 5694 – 5706.

[4] S. W. Kohl, F. W. Heinemann, M. Hummert, H. Weißhoff, A. Grohmann *Eur. J. Inorg. Chem.* **2006**, 3901 – 3910.

[5] S. W. Kohl, F. W. Heinemann, M. Hummert, W. Bauer, A. Grohmann *Dalton Trans.* **2006**, 5583 – 5592.

[6] A. Grohmann *Adv. Inorg. Chem.* **2004**, *56*, 179 – 210.

[7] C. Zimmermann, F. W. Heinemann, A. Grohmann *Eur. J. Inorg. Chem.* **2005**, 3506 – 3512.

[8] Y. Wakatsuki, H. Yamazaki *Synthesis* **1976**, 26 – 28.

[9] H. H. Karsch, A. Appelt *Z. Naturforsch.* **1983**, *38b*, 1399 – 1405.

[10] A. Trenkle, H. Vahrenkamp *Inorg. Synth.* **1982**, *21*, 180 – 181.

[11] R. Uriarte, T. J. Mazanec, K. D. Tau, D. W. Meek *Inorg. Chem.* **1980**, *19*, 79 – 85.

[12] K. Issleib, A. Tzschach *Chem. Ber.* **1959**, *92*, 704 – 711.

[13] G. W. Parshall *Inorganic Syntheses* **1968**, *11*, 157.

[14] L. Lassalle, S. Legoupy, J.-C. Guillemin *Organometallics* **1996**, *15*, 3466 – 3469.

[15] M. Stankevič, K. M. Pietrusiewicz *J. Org. Chem.* **2007**, *72*, 816 – 822.

[16] D. R. Lide *Handbook of Chemistry and Physics*, 86th ed., CRC Press, Boca Raton/USA, **2005**.

[17] G. Socrates *Infrared Characteristic Group Frequencies*, 2nd ed., Wiley, New York, **1994**.

[18] P. v. d. Sluis, A. L. Spek *Acta Crystallogr.* **1990**, *A46*, 194 – 201.